

Wireless Digital Control of Continuous Passive Plants Over Token Ring Networks

Nicholas Kottenstette¹, and Panos J. Antsaklis²

¹*Institute for Software Integrated Systems
Vanderbilt University
Nashville, TN 37203*

Email: nkottens@isis.vanderbilt.edu

²*Department of Electrical Engineering
University of Notre Dame
Notre Dame, IN 46556
Email: antsaklis.1@nd.edu*

SUMMARY

In a recent paper we have shown how *wave variables* can be used to interconnect *passive* plants with *passive* controllers such that the system remains l^2 -stable in spite of time varying delays and data dropouts. The present paper further enhances these results by providing a detailed model which captures time varying delays, data dropouts and network capacity for wireless ring token networks. It also provides a new theorem showing how an asynchronous controller can be implemented which maintains an l^2 -stable system. Simulations, show that asynchronous control of a *passive* motor reduces the overall distortion when compared to a synchronous controller which relies on lossy data reduction techniques. These two distinct results pave the way to study high performance rate adaptive control schemes which minimize their control rate in order to match the network capacity. Copyright © 2008 John Wiley & Sons, Ltd.

KEY WORDS: *passivity*, non-linear control, Markov chains, *Passive Asynchronous Transfer Unit, PATRU*, wave variables, switched systems, queuing theory, networked control, CC2420, 802.15.4

1. Introduction

In [13, Theorem 4] it has been shown how to digitally control a *passive* (Definition 6-i) plant over a network in which data can be subject to arbitrary time delays and data dropouts while remaining l^2 -stable. Initial simulations in [13] showed the system to perform quite well under fixed time delays however it remained to be shown how well the system performed under time varying delays. One similar class of control networks which has been extensively studied is that related to telemanipulation [1, 2, 14, 19, 20]. The purpose of this paper is twofold: first, to present a model which accurately captures

*Correspondence to: Institute for Software Integrated Systems
Vanderbilt University
Nashville, TN 37203

both the time varying delays associated with routing data over a token network and the data dropouts that occur due to finite queue length; and second, is to compare how well a *passive* asynchronous controller compares to a rate adaptive *passive* compression scheme [11, Section 4.3.1]. In order to evaluate performance we compare how our control scheme is able to effectively minimize the distortion (Definition 3) between a desired set point and the plants position through a simulated example. Since most digital control systems are concerned with sampling at a constant bit rate (*CBR*) we will focus our analysis on such *CBR* generating sources.

The networking delays and data dropout rate is intimately linked to the data rate of a *CBR* source, the length of the data queue and the capacity of the network. The capacity of the network is typically limited by the distance between stations, the radio, medium access control (*MAC*) and routing policy chosen. Therefore, much work has been done in order to determine optimum ways to route messages from various sources to desired sinks. In [25] classical optimal control techniques [16] were used to determine an optimal static routing policy which minimizes energy consumption. [18] provides an algorithm which specifies the nodes' order of transmission and power level in order to maximize the network lifetime known as *maximum lifetime accumulative broadcast (MLAB)*. [9] illustrates how to use feedback techniques in order to find the optimal number of redundant packets to send in order to maximize an objective function $J(u_b, n, p)$. [8] shows how to use feedback to control uncooperative users of networking resources. Unfortunately, most of these analysis are not concerned with attempting to characterize or understand the effects of the delay of the information transmitted in the network.

One paper which provides a model which captures round trip delays and data drop outs of small UDP packets sent over the Internet is presented in [5]. The model consists of a simple single server queueing model with two input streams, where one stream represents the probe traffic and the other stream represents the Internet traffic. Papers which look specifically at *MAC* protocols typically have a stronger relationship between network capacity and routing delays. Two popular wireless *MAC* protocols which have received much attention are m-phase time division multiple access (*TDMA*), and *ALOHA*. *TDMA* typically achieves a greater capacity than random access protocols such as *ALOHA*, however, for correlated flows such as those under a constant bit rate source (*CBR*), *ALOHA* can obtain greater capacity than *TDMA* [27]. Also, in [28] the time varying delay statistics can be computed for *TDMA* and *ALOHA MACs* subject to various sources such as a *CBR* source. These papers, do not characterize the delay characteristics for round trip communication patterns which will be seen in the l^2 -stable *passive* networks introduced in [13]. These networks can contain *passive* elements such as nonlinear n-DOF robots, such as those described in [2] which are used in telemanipulation systems [19]. Therefore, we shall study a simple token passing *MAC* protocol which will allow us to compute the network capacity and delays for our l^2 -stable *passive* networks.

In Section 2 we determine the delay characteristics of *MACs* which use token passing by developing the appropriate Markov chains to describe the system. The token ring network consists of m stations in which a station can only transmit new information to its successor if it currently possess a token received from its predecessor. Such a model is convenient as it allows us to focus our analysis on the head of queue delay of station m which generates new data packets at a constant packet rate r and still account for random communication delays incurred when relaying the data over the wireless networks remaining $m - 1$ stations. As such, the capacity of our network is calculated from the average number of round trip steps $\tau_m = \{M_m[v]\}$ taken for the delivery of control data which originated from the starting station m . τ_m is calculated using a convenient set of formulas provided by [22] and summarized in [11, Appendix C.1]. Note that a wireless token ring protocol was chosen to control the spacing of vehicles in the Automated Highway System program and the Berkeley Aerobot Project [7]. This protocol is robust and can handle problems such as duplicate tokens, lost stations (nodes), and

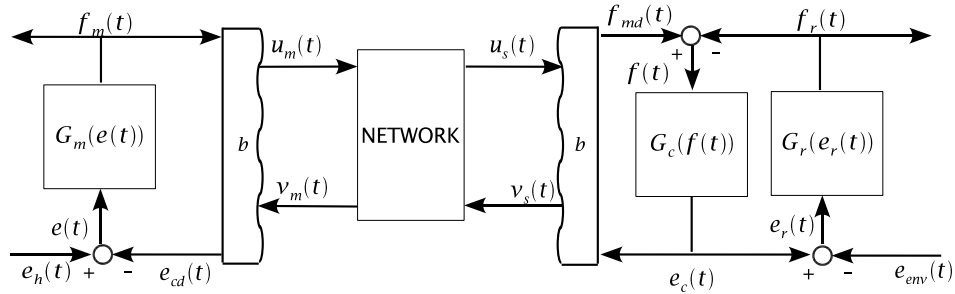


Figure 1. A telemanipulation system with flow-effort (velocity-force) architecture.

dynamically adding new stations to the ring. Furthermore, if m is large, smaller rings of stations could be established with an alternating carrier frequency in order to increase network capacity. In Section 2 we provide the basic analysis of a single ring of m stations. Looking at performance of a single ring is further justified when looking at potential wireless telesurgery applications in which $m = 4$, consisting of a station at the operator, robot and an aerial unmanned autonomous vehicle (the aerial vehicle can be treated as two stations in the ring) [20].

In [14] methods to reduce the data communicated over a network using sample based lossy data reduction (*LDR*) for telemanipulation systems has been investigated. It is concerned with developing *LDR* algorithms which provide good compression while attempting to maintain a high level of *transparency*. They proposed a measure which could be reflective of *transparency* which is computed by

$$I = \int_0^t [(f_m(\tau) - f_{md}(\tau))^2 + (e_c(\tau) - e_{cd}(\tau))^2] d\tau. \quad (1)$$

Comparing Figure 1 to [14, Fig. 2] we see that the flows (f_m, f_{md}) are treated as velocities (v_{hsi}, v_{to}) of the human system interface (*HSI*, $G_m(e(t))$) and teleoperator (*TO*) which consists of the controller $G_c(f(t))$ and robot $G_r(e_r(t))$. Likewise, the efforts (e_c, e_{cd}) represent the corresponding forces (F_{to}, F_{hsi}) depicted in [14, Fig. 2].

We are interested in evaluating the performance of our plant G_p controller G_c network as governed by the discrete random delays which occur over a wireless ring network. In Section 3 we will study the resulting distortion between a desired position set point $\theta_{set}(i)$ and the resulting position output from the plant $\theta_{act}(i)$. In particular we will show how a *novel passive* asynchronous control technique, in which the controller is only run when new data is received from the plant, outperforms a *passive* discrete time varying *LDR* algorithm [11, Section 4.3.1]. When the asynchronous controller is not running, it will drop the current reference input and its output will reset to 0 after being held at its last computed level for a period equal to that of the sample and hold period of the plant. Typically, when data for the controller is dropped over a *passive* control network, the controller either assumes a 0-input and updates its output accordingly or it attempts to make a prediction of what the correct input should be. The variable compression scheme compared attempts to make a smooth prediction on the input to tolerate delay and data dropouts. Although less steady state error and distortion occurs when using a variable compression scheme over a 0-input prediction scheme, it still does not perform as well as using an asynchronous controller for a simulated example. A detailed simulation and discussion is provided in Section 3.2 with a corresponding Theorem 1 (Section 3.3) which shows that the asynchronous controller is indeed *strictly-output passive*, as indicated by our simulations. Conclusions follow and

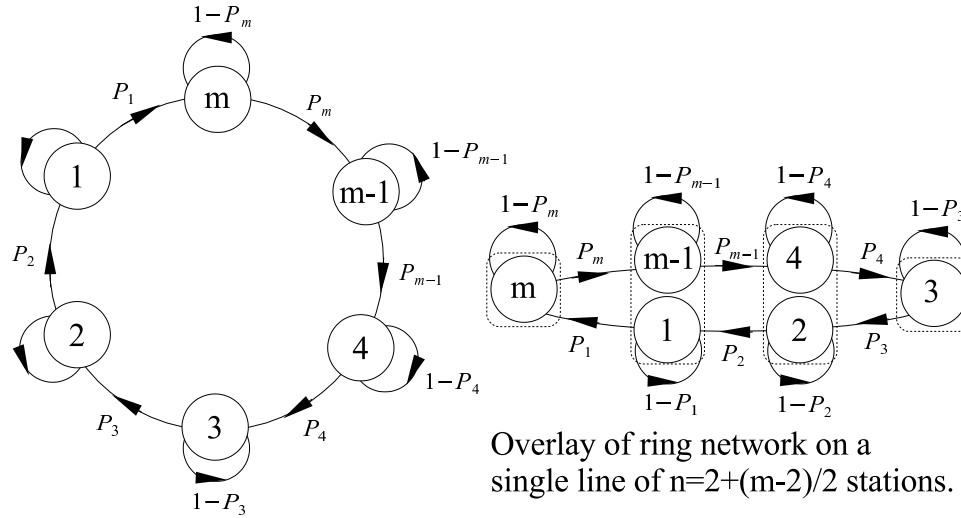


Figure 2. Ring networks consisting of m stations and $n = \frac{m-2}{2} + 2$ stations.

are presented in Section 4.

2. Capacity and Delay of Single Ring Token Networks

A ring network consists of m stations in which each station has a successor (the station it will pass its token to) and a predecessor (the station it will receive a token from). For simplicity we will consider rings in which station i will have the following predecessor, successor pairs $(pr_i, sc_i), \forall i \in \{1, \dots, m\}$:

$$(pr_i, sc_i) = \begin{cases} (i + 1, m), & \text{if } i=1; \\ (1, m - 1), & \text{if } i=m; \\ (i + 1, i - 1), & \text{otherwise.} \end{cases} \quad (2)$$

Figure 2 illustrates a corresponding ring network in which each station has a probability P_i of successfully sending a packet of n_p bits (which typically includes n_d data bits, n_h header bits and n_{fcs} frame check sequence bits) and receiving an acknowledgment of n_{ack} from its successor. For simplicity we assume that the successful transmission of a packet and receiving an acknowledgment is equivalent to passing a token to its successor. The packet dropout rate is denoted as P_{per} which is derived from the bit error rate P_{ber} such that $P_{per} = 1 - (1 - P_{ber})^{n_p}$ ([11, Appendix C.2]). Therefore, we conservatively estimate $P_i = (1 - P_{ber})^{n_p + n_{ack}}$. This assumption is conservative, since most people neglect the acknowledgment entirely.

Definition 1. Let the index $k = \{0, 1, 2, \dots\}$ denote a packet time slot, and let $x(k) = 1$ if a packet has been generated at station m at time k and let $x(k) = 0$ otherwise. If station m generates a packet of data to transmit around a ring network as depicted in Figure 2 at a constant packet rate r then it is

assumed that $x(k)$ behaves as follows:

$$x(k) = \begin{cases} 1, & \text{if } k \bmod r = 0. \\ 0, & \text{otherwise.} \end{cases} \quad (3)$$

In order for station m to transmit the new packet of data around the ring, it will need access to the token. Assume for simplicity, that the token is available at k then the soonest the next available token could arrive back at station m is $k + m$. Therefore, the minimum ideal rate in which station m can generate a packet is $r_{pc} = m$. Therefore, we define the ideal packet capacity as

$$\lambda_{pc} = \frac{1}{r_{pc}} = \frac{1}{m} \quad (4)$$

The average packet capacity λ_p depends on the average round trip time τ_m and has the following form

$$\lambda_p = \frac{1}{\tau_m} \quad (5)$$

In order to calculate τ_m we note that the following Markov chain describes a single packet journey in our ring network from station m and back to m . We capture the final round trip packet delivery from station 1 to station m with the corresponding absorbing state 0. The transition matrix P is as follows:

$$P = \begin{bmatrix} 1 & 0 & 0 & 0 & \dots & 0 \\ P_1 & 1 - P_1 & 0 & 0 & \dots & 0 \\ 0 & P_2 & 1 - P_2 & 0 & \dots & 0 \\ \dots & \dots & \dots & \dots & \dots & \dots \\ 0 & \dots & \dots & 0 & P_m & P_m - 1 \end{bmatrix} = \begin{bmatrix} I & \mathbf{0} \\ R & Q \end{bmatrix} \quad (6)$$

This is in canonical form [11, Appendix C.1]. We can now compute \mathbf{N} in which each $N_{i,j}$ element $i, j \in \{1, \dots, m\}$ is the average number of times each station j is visited if the packet originated in station i before the token reaches the absorbing state 0.

$$\mathbf{N} = (I - Q)^{-1} \quad (7)$$

$$\mathbf{N} = \begin{bmatrix} \frac{1}{P_1} & 0 & \dots & 0 \\ \frac{1}{P_1} & \frac{1}{P_2} & 0 & \dots & 0 \\ \frac{1}{P_1} & \frac{1}{P_2} & \frac{1}{P_3} & 0 & \dots & 0 \\ \dots & \dots & \dots & \dots & \dots & \dots \\ \frac{1}{P_1} & \frac{1}{P_2} & \frac{1}{P_3} & \dots & \dots & \frac{1}{P_m} \end{bmatrix} \quad (8)$$

Using the formulas in Table III the mean arrival time to station m when the initial packet started at station i is obtained by solving for τ :

$$\tau = \begin{bmatrix} \frac{1}{P_1} \\ \frac{1}{P_1} + \frac{1}{P_2} \\ \vdots \\ \sum_{i=1}^m \frac{1}{P_i} \end{bmatrix} \quad (9)$$

Or equivalently

$$\tau_i = \begin{cases} \frac{1}{P_i}, & i = 1; \\ \tau_{i-1} + \frac{1}{P_i}, & 1 < i \leq m. \end{cases} \quad (10)$$

Using (47) to solve for $\sigma_v^2 = \{\sigma_{v_i}^2\}$ (in which $\sigma_{v_i}^2$ represents the i^{th} element in vector σ_v^2 which describes the variance in arrival time to station m when the packet originated from station i) results in the following:

$$\sigma_{v_i}^2 = 2 \sum_{j=1}^i \frac{\tau_j}{P_j} - \tau_i(1 + \tau_i). \quad (11)$$

Solving for $\sigma_{v_\delta}^2 = (\sigma_{v_i}^2 - \sigma_{v_{i-1}}^2)$ results in the following:

$$\sigma_{v_\delta}^2 = \frac{2\tau_i}{P_i} - \tau_i(1 + \tau_i) + \tau_{i-1}(1 + \tau_{i-1}) \quad (12)$$

$$= \frac{2\tau_i}{P_i} - \tau_i - \tau_i^2 + \left(\tau_i - \frac{1}{P_i}\right)\left(1 + \tau_i - \frac{1}{P_i}\right) \quad (13)$$

$$= \frac{1 - P_i}{P_i^2}. \quad (14)$$

Therefore, $\sigma_{v_i}^2$ can be equivalently written in the following recursive form

$$\sigma_{v_i}^2 = \begin{cases} \frac{1-P_1}{P_1^2}, & \text{if } i = 1; \\ \sigma_{v_{i-1}}^2 + \frac{1-P_i}{P_i^2}, & 1 < i \leq m. \end{cases} \quad (15)$$

We now state the following lemma.

Lemma 1. *Given a ring network as described by (2) and depicted in Figure 2. In which each station $i \in \{1, \dots, m\}$ has a probability P_i of successfully sending a message to its successor station and $1 - P_i$ of unsuccessfully sending the message per attempt, the following holds:*

- i. *The average steps it takes to relay a message from station m around the ring network is $\tau_m = \sum_{i=1}^m \frac{1}{P_i}$, for the special case $P_i = p$ then $\tau_m = \frac{m}{p}$.*
- ii. *The corresponding variance in the round trip time is $\sigma_{v_m}^2 = \sum_{i=1}^m \frac{1-P_i}{P_i^2}$, for the special case $P_i = p$ then $\sigma_{v_m}^2 = \frac{m(1-p)}{p^2}$.*

Remark 1. *The corresponding packet capacity of the ring network is $\lambda_p = \frac{1}{\tau_m}$, for the special case $P_i = p$ then $\lambda_p = \frac{p}{m}$. The solution of λ_p is a direct substitution of $\tau_m = \frac{m}{p}$ (Lemma 1-i) into (5) from Definition 1.*

Proof 1. *Most of the proof has been provided in the subsequent discussion. In summary:*

- i. *The solution for τ_m is provided by (9).*
- ii. *The solution for $\sigma_{v_m}^2$ is easily obtained by our recursive solution given by (15).*

Remark 2. *For the l^2 -stable digital control network depicted in Figure 7 with $n - 2$ equally spaced relay nodes, we can create a ring network as depicted in Figure 2 in which station m contains the plant G_p and station $\frac{m}{2} = n - 1$ contains the controller G_c . Furthermore assume that $P_i = p, \forall i \in \{1, 2, \dots, m\}$. Then the average packet transmission delay ($E\{p(i)\}$) from plant to controller station and from controller to plant station ($E\{c(i)\}$) is $\frac{m}{2p} = \frac{n-1}{p}$ with a corresponding variance of $\frac{(n-1)(1-p)}{p^2}$.*

Although, the packet capacity is a convenient abstraction for characterizing the network, we still need to quantify the actual rate of data being transmitted. Therefore, we provide the following definition:

Definition 2. *The data capacity of a ring network is the number of actual data bits per second which can be transmitted round trip from a given source node, in which the data is relayed from every station in the network. Therefore, the data capacity in the ring network is*

$$\lambda_d = \frac{f_{bit}\lambda_p n_d}{(n_p + n_{ack})} \quad (16)$$

in which λ_p is the packet capacity, n_d is the number of actual data bits which get transmitted for a successful packet delivery, n_p is the number of packet bits, n_{ack} is the number of bits required for the acknowledgment, and f_{bit} is the transmit data rate (bits per second).

For the special case when each node is equally spaced in a line network with n nodes ($m = 2(n - 1)$ stations) then the corresponding data capacity is

$$\lambda_d = \frac{f_{bit}n_d p}{m(n_p + n_{ack})} = \frac{f_{bit}n_d p}{m(n_d + n_h + n_{fcs} + n_{ack})} \quad (17)$$

in which p is dependent on n_p , and n_{ack} and the node spacing d . This dependency is seen, as we recall that

$$p = 1 - P_{per} = (1 - P_{ber})^{n_p + n_{ack}},$$

in which the probability of a bit error $P_{ber} = f(\text{snr})$ depends on the received signal to noise ratio (snr). In which the received signal to noise ratio depends on the radio and transmission path loss $P_L(d)$ which is a function of the node spacing d and the transmission path loss model chosen [11, Appendix C.2]. The CC2420 is a true single-chip 2.4 GHz IEEE 802.15.4 compliant RF transceiver designed for low power and low voltage wireless applications [10]. Building from the analysis provided in [11, Appendix C.2] for determining the packet error rate for the CC2420 and using the following parameters given in Table I: we can calculate λ_d as a function of d and n_d in which $m\lambda_d$ is plotted

Table I. CC2420 PARAMETERS SUMMARY.

Term	Symbol	Value
bits per second	f_{bit}	250×10^3 bps
header bits	n_h	$13 * 8 = 104$ bits
frame check sequence bits	n_{fcs}	$2 * 8 = 16$ bits
ack bits	n_{ack}	$11 * 8 = 88$ bits
data bits	n_d	$0 \leq n_d \leq 960$ bits
typical transmit power	P_T	$-24 \leq P_T \leq 0$ dBm
worst case transmit power	P_T	$-27 \leq P_T \leq -3$ dBm
typical noise figure	NF	15.44 dB
worst case noise figure	NF	20.44 dB

in Figure 3(a) and $d \times m \times \lambda_d$ is plotted in Figure 3(b). These are fairly easy estimates to remember and use when attempting to determine the average delays in a ring network. However, there is a way to get an even closer estimate of the corresponding delay in the network. Using techniques similar to those used by [15, 26], we describe a two dimensional Markov chain to track the head of queue *HoQ* delay at station m for an outgoing packet which is generated from a *CBR* source which generates

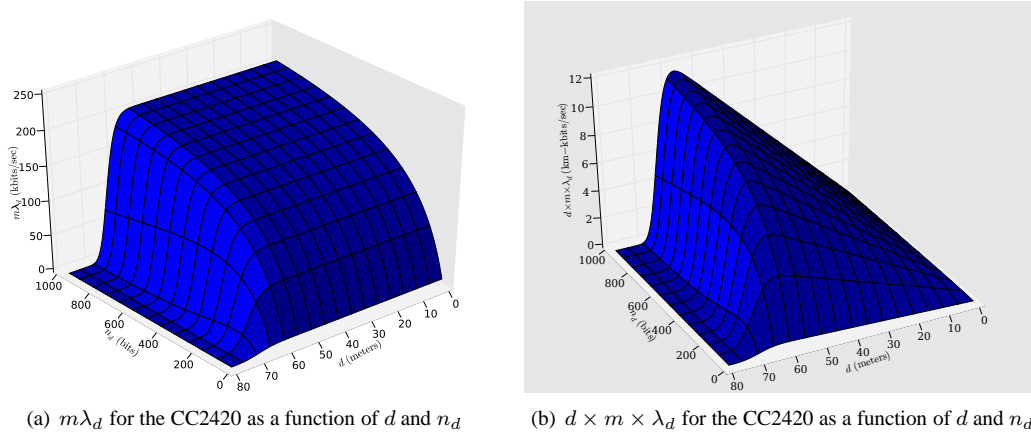


Figure 3. Normalized network capacity plots assuming $n = 3.3$, $d_o = 8$ meters, $P_T = -3$ dBm, $NF = 20.44$ dB.

packets at packet rate r to be transmitted over a token ring network. The chain will be described by the $(d(k), s(k))$ tuple (or more compactly (d, s)) in which $d(k) \in \{-r + 1, -r + 2, \dots, D\}$ denotes the delay of the HoQ at packet time slot k in which D is the maximum delay before the packet will be dropped or compressed and $s(k) \in \{1, 2, \dots, m\}$ is the station where the token is in the network at time k . In particular the HoQ delay, $d(k)$ is related to the packet generation rate r as follows:

$$d(k + 1) = d(k) - (\theta(k)r - 1). \quad (18)$$

in which

$$\theta(k) = \begin{cases} 1, & \text{if station } m \text{ has a token } s(k) = m \text{ and transmits the token to station } m - 1 \text{ (s(k+1)=m-1).} \\ 0, & \text{otherwise.} \end{cases}$$

Note, that when $d(k) < 0$ it indicates that there is no data in the transmit buffer of station m in addition the next packet will be generated at time $(k - d(k))$ i.e. $(x(k - d(k)) = 1)$. Note that for the simple example given in Table II it is impossible for the delay of the head of queue to be reduced to 0 without flushing the queue, even if the token was successfully passed between station 1 and station 2 for all remaining $k > 10$.

Table II. A simple example illustrating (18), when $r = 2$ and $m = 2$.

k	0	1	2	3	4	5	6	7	8	9	10
$x(k)$	1	0	1	0	1	0	1	0	1	0	1
$s(k)$	2	1	2	1	1	2	1	2	1	2	2
$\theta(k)$	1	0	1	0	0	1	0	1	0	0	1
$d(k)$	0	-1	0	-1	0	1	0	1	0	1	2

Lemma 2. Given a ring network as described by (2) and depicted in Figure 2 and assuming that a packet (of n_p bits) will be rotated through the network (even if no new data is present). In which each station $i \in \{1, \dots, m\}$ has a probability P_i of successfully sending a message to its successor

station and $1 - P_i$ of unsuccessfully sending the message per attempt, the following transition matrix $P \in \mathbb{R}^{((D+r)m) \times ((D+r)m)}$ describes the HoQ delay:

$$P = \begin{matrix} & \begin{matrix} (-r+1, s) \\ (-r+2, s) \\ \dots \\ (-1, s) \\ (0, s) \\ (1, s) \\ \dots \\ (D-1, s) \\ (D, s) \end{matrix} & \begin{bmatrix} \mathbf{0} & \mathbf{P}_r & \mathbf{0} & \dots & \mathbf{0} \\ \mathbf{0} & \mathbf{0} & \mathbf{P}_r & \mathbf{0} & \dots & \mathbf{0} \\ \dots & \dots & \dots & \dots & \dots & \dots \\ \mathbf{0} & \mathbf{0} & \dots & \mathbf{0} & \mathbf{P}_r & \mathbf{0} & \dots & \mathbf{0} \\ \mathbf{P}_m & \mathbf{0} & \dots & \mathbf{0} & \mathbf{P}_r - \mathbf{P}_m & \mathbf{0} & \dots & \mathbf{0} \\ \mathbf{0} & \mathbf{P}_m & \mathbf{0} & \dots & \mathbf{0} & \mathbf{0} & \mathbf{P}_r - \mathbf{P}_m & \mathbf{0} \\ \dots & \dots & \dots & \dots & \dots & \dots & \dots & \dots \\ \mathbf{0} & \dots & \mathbf{0} & \mathbf{P}_m & \mathbf{0} & \dots & \mathbf{0} & \mathbf{P}_r - \mathbf{P}_m \\ \mathbf{0} & \dots & \mathbf{0} & \mathbf{P}_r & \mathbf{0} & \dots & \mathbf{0} & \mathbf{0} \end{bmatrix} \end{matrix} \quad (19)$$

in which $\mathbf{P}_r \in \mathbb{R}^{m \times m}$ is the transition matrix which describes the evolution of the token,

$$\mathbf{P}_r = \begin{bmatrix} 1 - P_1 & 0 & \dots & 0 & P_1 \\ P_2 & 1 - P_2 & 0 & \dots & 0 \\ 0 & P_3 & 1 - P_3 & 0 & \dots & 0 \\ \dots & \dots & \dots & \dots & \dots & \dots \\ 0 & \dots & 0 & P_{m-1} & 1 - P_{m-1} & 0 \\ 0 & \dots & 0 & P_m & 1 - P_m \end{bmatrix} \quad (20)$$

and $\mathbf{P}_m \in \mathbb{R}^{m \times m}$ is the part of the transition matrix which captures shrinking of the HoQ delay from d to $d - r + 1$ when the token is at station m and is successfully transmitted to station $m - 1$

$$\mathbf{P}_m = \begin{bmatrix} 0 & 0 & 0 & 0 \\ 0 & \dots & 0 \\ 0 & \dots & 0 \\ \dots & \dots & \dots \\ 0 & \dots & 0 \\ 0 & 0 & P_m & 0 \end{bmatrix}. \quad (21)$$

The (\mathbf{d}, \mathbf{s}) is a short hand to show how the states of the chain correspond to the rows of the transition matrix P in which d is a fixed column of integers and s would have each row correspond to the next state in the chain describing the evolution of the token i.e.

$$(\mathbf{d}, \mathbf{s}) = \begin{matrix} (d, 1) \\ (d, 2) \\ (d, 3) \\ (\cdot, \cdot) \\ (d, m - 1) \\ (d, m) \end{matrix}. \quad (22)$$

Proof 2. The transition matrix P as described by (19) consists of combinations of $m \times m$ block matrices $\{\mathbf{0}, \mathbf{P}_r, \mathbf{P}_m\}$. Assuming that north is the top of the page and south the bottom of the page we will use the following notation to indicate the location of each block matrix within P as $P(x, y)$ in which: $P(-r + 1, -r + 1)$ represents the most north-west block; $P(D, -r + 1)$ represents the most south-west block; $P(-r + 1, D)$ represents the most north-east block; finally, $P(D, D)$ represents the most south-east block.

1. $(-r + 1) \leq d < 0, s \in \{1, \dots, m\}$: \mathbf{P}_r describes the evolution of the token $s(k)$. Since there is no packet in the HoQ, $\theta(k) = 0$, which when substituted into (18) results in

$$d(k + 1) = d(k) + 1, \forall s(k) \in \{1, 2, \dots, m\}.$$

Therefore for the case when $x \in \{-r + 1, -r + 2, \dots, -1\}$

$$P(x, y) = \begin{cases} \mathbf{P}_r, & \text{if } y = (x + 1) \\ \mathbf{0}, & \text{otherwise.} \end{cases}$$

2. $0 \leq d(k) < D, s(k) \in \{1, \dots, m\}$: once the HoQ delay $d(k) \geq 0$, a packet is available for transmission at station m , hence if station m has the token and successfully transmits to station $m - 1$ then $\theta(k) = 1$, otherwise $\theta(k) = 0$. Therefore, from (18) the delay $d(k)$ will evolve as follows

$$d(k + 1) = \begin{cases} d(k) - (r - 1), & \text{if } s(k) = m \text{ and } s(k + 1) = (m - 1) \\ d(k) + 1, & \text{otherwise.} \end{cases}$$

When $s(k) = m$, a successful transmission ($s(k + 1) = (m - 1)$) will occur with probability P_m which is used in formulating the matrix \mathbf{P}_m . Conversely, token transmissions from any other station will have $\theta(k) = 0$ in which the delay d will increase by one, therefore $\mathbf{P}_r - \mathbf{P}_m$ will describe the remaining state transitions which do not lead in reducing the HoQ delay. Therefore, for the case when $x \in \{0, 1, \dots, D - 1\}$

$$P(x, y) = \begin{cases} \mathbf{P}_m, & \text{if } y = (x - r + 1) \\ \mathbf{P}_r - \mathbf{P}_m, & \text{if } y = (x + 1) \\ \mathbf{0}, & \text{otherwise.} \end{cases}$$

3. $d(k) = D, s(k) \in \{1, \dots, m\}$: once the delay $d(k) = D$ the packet will either be successfully delivered or dropped ($\theta(k) = 1$), therefore, the delay will shrink such that

$$d(k + 1) = D - (r - 1), \forall s(k) \in \{1, 2, \dots, m\}.$$

Thus, we only need to track the evolution of the token s which is described by \mathbf{P}_r . Therefore,

$$P(D, y) = \begin{cases} \mathbf{P}_r, & \text{if } y = (D - r + 1) \\ \mathbf{0}, & \text{otherwise.} \end{cases}$$

Remark 3. Noting that the Markov chain evolves according to

$$\pi(k + 1) = \pi(k)P. \quad (23)$$

Then in order to calculate the average delay of the HoQ we simply solve for the steady state distribution of our Markov chain

$$\pi P = \pi, \quad (24)$$

in which $\pi = (\pi_{(-r+1,1)}, \pi_{(-r+1,2)}, \dots, \pi_{(-r+1,m)}, \pi_{(-r+2,1)}, \dots, \pi_{(D,m)})$ is a row vector. The delay distribution, $d_i (0 \leq d \leq D)$ is given by

$$d_i = \frac{P_m \pi_{(i,m)}}{\sum_{k=0}^D P_m \pi_{(k,m)}} = \frac{\pi_{(i,m)}}{\sum_{k=0}^D \pi_{(k,m)}} \quad (25)$$

where $\sum_{k=0}^D P_m \pi_{(k,m)}$ is the normalizing constant, in which we only consider successful transmissions with probability P_m from station m to station $m - 1$ in deriving the delay distribution.

Remark 4. Calculating the packet loss probability p_o is simply

$$\begin{aligned} p_o &= \frac{(1 - P_m)\pi_{(D,m)} + \sum_{k=1}^{m-1} \pi_{(D,k)}}{\lambda} \\ &= r[(1 - P_m)\pi_{(D,m)} + \sum_{k=1}^{m-1} \pi_{(D,k)}] \end{aligned} \quad (26)$$

in which $\lambda = \frac{1}{r}$, if we are in any other state besides m the packet will be dropped, when in state m there is only a probability of $(1 - P_m)$ of dropping the packet and that is accounted for.

Remark 5. For the l^2 -stable digital control network depicted in [13, Fig. 2] with $n - 2$ equally spaced relay nodes, we can create a ring network as depicted in Figure 2 in which station m is the plant G_p and station $\frac{m}{2} = n - 1$ is the controller G_c . The controller only returns control data if it has received data from the plant. If we consider the queuing delay associated with a CBR source at m and consider that the controller will not immediately compute a control command but pass along computations from previous transmissions. Then we can more closely approximate the delay of the delivery of data from the controller to the plant as if it was provided a CBR source r as well. This average delay from G_p to G_c and vice versa can be computed as follows:

$$\tau_{pc} = \sum_{i=1}^D id_{p_i} + \sum_{i=m-1}^{\frac{m}{2}-1} \frac{1}{P_i} \text{ for the delay from } G_p \text{ to } G_c, \quad (27)$$

$$\tau_{cp} = \sum_{i=1}^D id_{c_i} + \sum_{i=\frac{m}{2}}^{m-1} \frac{1}{P_i} \text{ for the delay from } G_c \text{ to } G_p \quad (28)$$

in which d_{x_i} is the corresponding delay distribution for either the plant or controller if they were supplied a CBR source r . If $P_i = p$ then $\tau_{pc} = \tau_{cp}$ such that

$$\tau_{pc} = \tau_{cp} = \sum_{i=1}^D id_i + \frac{(m-2)}{2p} \quad (29)$$

and the corresponding variance is

$$\sigma_v^2 = \sum_{i=1}^D i^2 d_i - \left(\sum_{i=1}^D id_i\right)^2 + \frac{(n-2)(1-p)}{p^2}. \quad (30)$$

3. Distortion in Single Ring Token Networks

We have characterized the delay in Section 2, however, in order to account for the time varying queuing delay we assume that when the delay exceeds D slots the data packet should be dropped. However, dropping packets may lead to drift in the actual position of the plant $\theta_{act}(i)$ when it is controlled using velocity feedback. Instead of dropping the data when it reaches the maximum delay D we chose to implement a *LDR* algorithm described in [11, Section 4.3.1] which is similar to the *compressor-expander* scheme used in [3, 4]. We use a distortion measure (Definition 3) in order to evaluate the performance of these compression schemes.

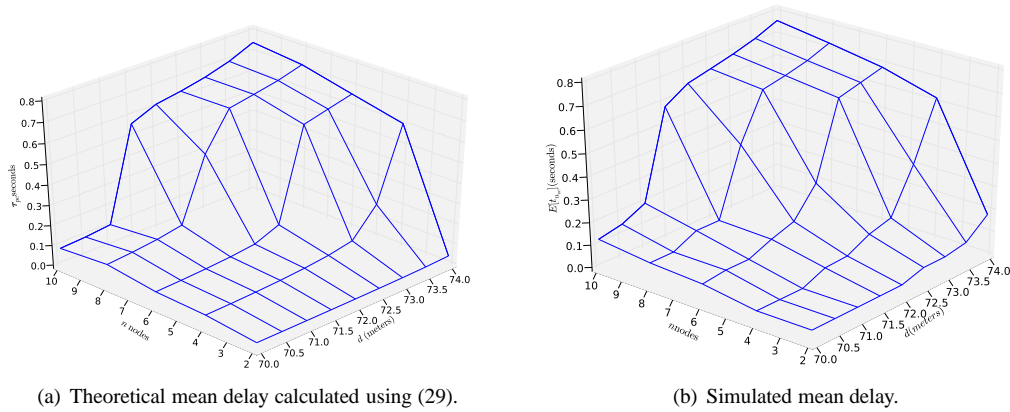


Figure 4. Theoretical and simulated mean delay of u_{oc} in which up to 240 bit samples of u_{oc} can be transmitted (maximum $n_p = 288$ bits, $S = -90$ dBm, $P_T = -3$ dBm, $n = 3.3$, $d_o = 8.0$ meters, maximum $r = 86$, $D = 516$).

Definition 3. Consider l^2 -stable digital control networks similar to those depicted in Figure 7 (with or without the PATRU) in which the flow output is denoted as $f_p(t)$. Denote the sampled integrated output of the plant as $\theta_{act}(i)$ which depends on the sampling rate T_s such that

$$\theta_{act}(i) = \int_0^{iT_s} f_p(t) dt.$$

Further, assume that the user will provide a desired set point $\theta_{set}(i)$ (with z -transform $\theta_{set}(z)$) to the input of a discrete second order trajectory generator $H_t(z)$ which is a zero-order hold equivalent of $H_t(s)$

$$H_t(s) = \frac{\omega_{traj}^2 s}{s^2 + 2\zeta\omega_{traj}s + \omega_{traj}^2}$$

such that

$$r_{oc}(z) = -H_t(z)\theta_{set}(z)$$

($r_{oc}(z)$ is the z -transform of $r_{oc}(i)$). The mean squared distortion is

$$I_\theta = \frac{1}{T} E \left\{ \sum_{i=0}^T (\theta_{set}(i) - \theta_{act}(i))^T (\theta_{set}(i) - \theta_{act}(i)) \right\} \quad (31)$$

in which $E[\cdot]$ denotes the expectation of the summation of the squared error which is dependent on the set point, the controller, the plant dynamics, and the time varying delays incurred due to the communication network.

In the subsequent discussion which follows we will compare the distortion results of a classic motor control problem described in [13, Section IV]. The motor to be controlled is characterized by its torque constant, $K_m > 0$, back-emf constant K_e , rotor inertia, $J_m > 0$, and damping coefficient $B_m > 0$.

The *passive* dynamics are described by

$$\dot{\omega} = -\frac{B_m}{J_m}\omega + \frac{K_m}{J_m}i. \quad (32)$$

We choose to use the *passive* "proportional-derivative" controller described by (33).

$$K_{PD}(s) = K \frac{\tau s + 1}{s} \quad (33)$$

Using loop-shaping techniques we choose $\tau = \frac{J_m}{B_m}$ and choose $K = \frac{J_m \pi}{10 K_m T_s}$. This will provide a reasonable crossover frequency at roughly a tenth the Nyquist frequency and maintain a 90 degree phase margin. We choose to use the same motor parameter values given in [17] in which $K_m = 49.13$ (mV \times rad \times sec), $J_m = 7.95 \times 10^{-3}$ (kg \times m²), and $B_m = 41$ (μ N \times sec/meter). With $T_s = .05$ seconds, we use [12, Corollaries 4,5] to synthesize a *strictly-output passive* plant and controller from our continuous model (33). We also use [12, Corollary 3] in order to compute the appropriate gains for both the controller $K_{sc} = 1$ and the *strictly-output passive* plant $K_{sp} = 20$.

In particular we will compare the resulting step response and corresponding distortion when adaptive compression is used as opposed to a novel asynchronous controller which only calculates a new control command when sensor data is received from the plant. We estimated the corresponding distortion by averaging the summation inside the expectation of (31) over 50 trials for a fixed number of n nodes and spacing of d meters. We chose $\theta_{set}(i)$ to use a square wave profile which is 0.0 radians for $0 \leq t < 8.0$ seconds, 1.0 radians for $8 \leq t < 16.0$ seconds, -1.0 radians for $16.0 \leq t < 24.0$ seconds, 0 radians for $24.0 \leq t$ seconds (Figure 6(a)). Since we chose a modest sampling rate of .05 seconds we generate data at $5 * 8 / .05 = 800.0$ bits per second. Which is a small fraction of the maximum data rate that can be achieved between a small number of nodes. As such, the delay between receiving data from the plant and controller is roughly the sampling rate (.05 seconds) for distances less than 70 meters.

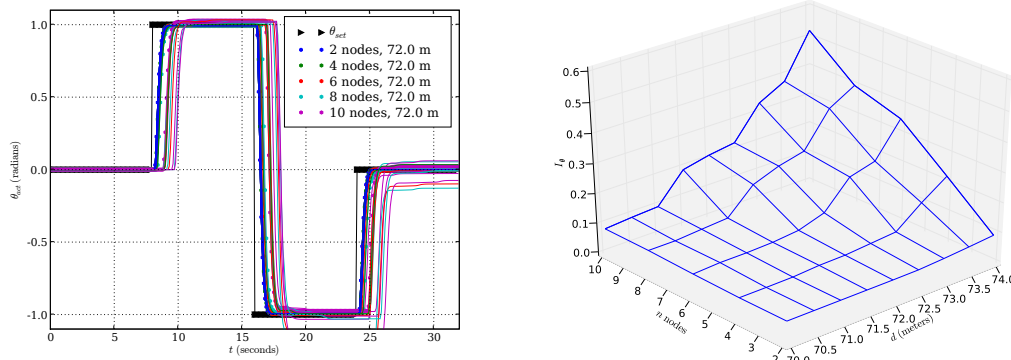
3.1. Summary of LDR results.

A detailed *LDR* algorithm is presented in [11, Section 4.3.1], and has been simulated for the motor control example. Figure 5(a) shows the typical step response under various m stations and station spacing d . The corresponding distortion is given in Figure 5(b). Note that when $I_\theta = 0.5$ can be achieved by simply keeping $\theta_{act} = 0$.

3.2. Comparing LDR Algorithm With Dropping Data in a Full First-In, First-Out (FIFO) buffer.

As we have seen, the *LDR* algorithm behaves exceptionally well for extremely unreliable communication channels. When the nodes are spaced 72.0 meters apart, the probability of a successful packet transmission is $P = (1.0 - .00631781)^{8 \times (11+2+13+2 \times 5)} = 16\%$. Which corresponds to a capacity of 5596 bits/second for two nodes, and 622 bits/second for ten nodes ($m = 18$). Thus, to maintain an effective 800 bit/second data rate for ten nodes the data needs a compression ratio of 800/622 and negligible distortion is seen. However, as the compression ratio increases so does the distortion in Figure 5(b), which is seen in the delay and resulting steady state errors in Figure 5(a). Although the step responses are fairly smooth, when the nodes are 74.0 meters apart the probability of a successful packet transmission is $P = (1.0 - .010108)^{8 \times (11+2+13+2 \times 5)} = 5.3\%$. Which corresponds to a capacity of 1861 bits/second for two nodes, and 207 bits/second for ten nodes ($m = 18$) with a required compression ratio nearing 4.

However, when a FIFO is full and if we choose to use no compression and either drop the oldest or the current data sample, we can reduce the distortion at the lower data rates. This was an *unexpected*



(a) Typical step responses using *LDR* algorithm for nodes of (b) Distortion for motor example in which $S = -90\text{dBm}$, 2, 4, 6, 8, 10 and transmission distances of 70, 70.5, 71, $P_T = -3\text{dBm}$, $n = 3.3$, $d_o = 8.0$ meters, each sample 71.5, 72.0, 72.5, 73.0, 73.5, 74 meters (each color in plot consists of 40 bits, and up to 2 samples will be transmitted if corresponds to a unique number of nodes). available in a single packet.

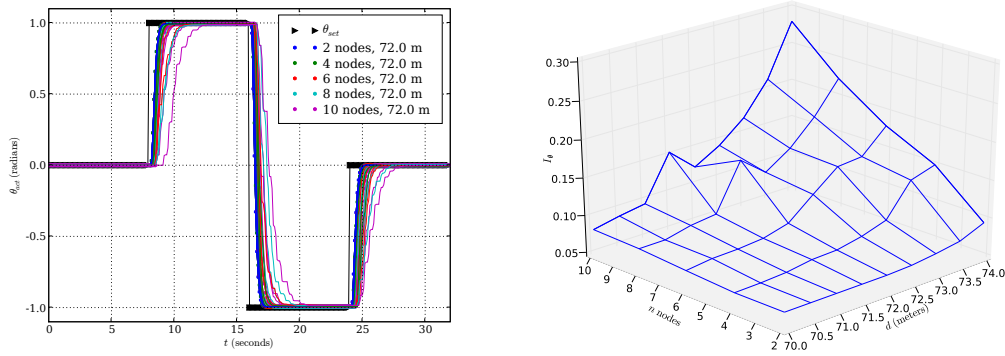
Figure 5. Step response and corresponding distortion using *LDR*.

result, after reading about previous simulations in which dropped data resulted in steady state error [4, Figure 9] [3, Figure 5, Figure 6]. However, we have been implementing our controller in a slightly different manner when not using compression. The controller only computes a new command when data from the plant is received, which implies we do not calculate a control command which will steer us away from our desired location by using a zero input. Furthermore, we achieved a significant improvement in distortion by simply dropping the sampled control input when data is not available from the plant. These two seemingly simple changes lead to a significant improvement in reducing distortion as can be seen in the step responses in Figure 6(a) and distortion plot in Figure 6(b).

3.3. Asynchronous Passivity

Figure 7 indicates how to implement a *passive* digital controller in an asynchronous manner. Let $z^{-p(i)}$ and $z^{-c(i)}$ represents a time varying delay element such that if the *PATRU* was bypassed and $i = j$, then $u_{oc}(i) = u_{op}(i - p(i))$ and $v_{op}(i) = v_{oc}(i - c(i))$ at time i in which $c(i)$ and $p(i)$ would be positive integers. The *IPES* and *ZOH* blocks are used to digitally control a continuous *passive* plant and are described in more detail in Appendix II.2. The wave variables depicted in Figure 7 ($u_{o\{p,c\}}(i)$, $v_{o\{p,c\}}(i)$) are also reviewed in Appendix II.3. The transfer of data between the controller and the plant is handled by the *Passive Asynchronous Transfer Unit (PATRU)*. **Note** that the controller only computes a new control command $e_{oc}(j)$ when new data arrives from the *PATRU* $u_{oc}(j)$, hence, why we refer to this as an asynchronous controller.

Definition 4. Define the set I as the set of received indexes $l = (i - p(i))$ from the plant which correspond to the received tuple $(l, u_{op}(l))$ and the set J as the set of received indexes $k = (i - c(i))$ from the controller (via the *PATRU*) which correspond to the received tuple $(k, v_{oc}(k))$. When the plant and controller are initially enabled the sets I and J are empty. For simplicity of discussion we assume that the controller can instantly compute a new control command e_{oc} when new data arrives from the



(a) Typical step response by dropping either the latest (b) Distortion plot by dropping either the latest sample or sample or current sample when FIFO is full for current sample when FIFO is full. nodes of 2, 4, 6, 8, 10 and transmission distances of 70, 70.5, 71, 71.5, 72.0, 72.5, 73.0, 73.5, 74 meters (each color in plot corresponds to a unique number of nodes).

Figure 6. Step response and corresponding distortion with asynchronous control and dropping latest sample.

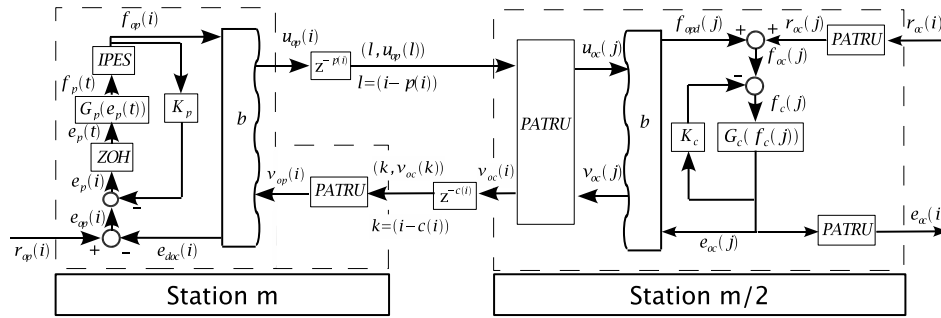


Figure 7. Passive digital control network with Passive Asynchronous Transfer Unit (PATRU).

plant. The PATRU then handles the transfer of data as follows:

1. If the periodically generated tuple $(l, u_{op}(l))$ from the plant has arrived to the PATRU on the controller side then:

if $l \in I^c$:

$$u_{oc}(j) = u_{op}(l)$$

$$r_{oc}(j) = r_{oc}(i)$$

$$I = l \cup I$$

calculate new $v_{oc}(j)$, and $e_{oc}(j)$

$$v_{oc}(i) = v_{oc}(j)$$

$$e_{oc}(i) = e_{oc}(j)$$

$$j = j + 1$$

else:

$$\begin{aligned} v_{oc}(i) &= 0 \\ e_{oc}(i) &= 0 \\ \text{transmit}(i, v_{oc}(i)) \end{aligned}$$

2. Otherwise if no periodically generated tuple $(l, u_{op}(l))$ from the plant has arrived to the PATRU on the controller side then:

$$\begin{aligned} v_{oc}(i) &= 0 \\ e_{oc}(i) &= 0 \\ \text{transmit}(i, v_{oc}(i)) \end{aligned}$$

3. If the periodically generated tuple $(k, v_{oc}(k))$ from the PATRU on the controller side has arrived to the PATRU on the plant side then:

$$\begin{aligned} \text{if } k \in J^c: \\ v_{op}(i) &= v_{oc}(k) \\ J &= k \cup J \end{aligned}$$

else:

$$\begin{aligned} v_{op}(i) &= 0 \\ \text{transmit}(i, u_{op}(i)) \end{aligned}$$

4. Otherwise if no periodically generated tuple $(k, v_{oc}(k))$ from the PATRU on the controller side has arrived to the PATRU on the plant side then:

$$\begin{aligned} v_{op}(i) &= 0 \\ \text{transmit}(i, u_{op}(i)) \end{aligned}$$

Using definition 4 we give the following lemma:

Lemma 3. Using the PATRU as defined by Definition 4,

$$\langle f_{op}(i), e_{doc}(i) \rangle_{N_i} \geq \langle e_{oc}(j), f_{opd}(j) \rangle_{N_j} \quad (34)$$

holds for all $N_i \in \{1, 2, \dots\}$ and $N_j \in \{1, 2, \dots\}$.

Proof 3. To begin, we note that $N_i > N_j$ since the controller will only process received data from the plant. From the wave variable transform we also know that (34) can be equivalently written as

$$\|(u_{op}(i))_{N_i}\|_2^2 - \|(v_{op}(i))_{N_i}\|_2^2 \geq \|(u_{oc}(j))_{N_j}\|_2^2 - \|(v_{oc}(j))_{N_j}\|_2^2. \quad (35)$$

It is sufficient for (35) to hold if both

$$\|(u_{op}(i))_{N_i}\|_2^2 \geq \|(u_{oc}(j))_{N_j}\|_2^2 \quad (36)$$

and

$$\|(v_{oc}(j))_{N_j}\|_2^2 \geq \|(v_{op}(i))_{N_i}\|_2^2 \quad (37)$$

hold. By definition 4 we know that $u_{oc}(j)$ can only consist of unique samples of $u_{op}(i)$ therefore (36) is obviously satisfied. Likewise, $v_{op}(i)$ can only consist of unique samples of $v_{oc}(j)$ or the value 0 therefore (37) is satisfied.

With lemma 3 we state the additional lemma which shows that using the PATRU an expression can be obtained which is sufficient for a strictly-output passive system when $i = j$.

Lemma 4. *Using the PATRU as defined by Definition 4 in the control network depicted in Figure 7. The following inequality is satisfied:*

$$\langle f_{op}(i), r_{op}(i) \rangle_{N_i} + \langle e_{oc}(j), r_{oc}(j) \rangle_{N_j} \geq \epsilon (\| (f_{op}(i))_{N_i} \|_2^2 + \| (e_{oc}(j))_{N_j} \|_2^2) - \beta \quad (38)$$

in which $\epsilon = \min(\epsilon_{op}, \epsilon_{oc})$ and $\beta = \beta_{op} + \beta_{oc}$. When $i = j$ the network is strictly-output passive.

The proof follows along the lines as the one provided for [13, Theorem 4].

Proof 4. *First, by [13, Theorem 3-I], G_p is transformed to a discrete passive plant. Next, by [13, Theorem 2] both the discrete plant and controller are transformed into strictly-output passive systems. The strictly-output passive plant satisfies*

$$\langle f_{op}(i), e_{op}(i) \rangle_{N_i} \geq \epsilon_{op} \| (f_{op}(i))_{N_i} \|_2^2 - \beta_{op} \quad (39)$$

while the strictly-output passive controller satisfies (40).

$$\langle e_{oc}(j), f_{oc}(j) \rangle_{N_j} \geq \epsilon_{oc} \| (e_{oc}(j))_{N_j} \|_2^2 - \beta_{oc} \quad (40)$$

Substituting, $e_{doc}(i) = r_{op}(i) - e_{op}(i)$ and $f_{od}(j) = f_{oc}(j) - r_{oc}(j)$ into (34) (which holds by Lemma 3) yields

$$\langle f_{op}(i), r_{op}(i) - e_{op}(i) \rangle_{N_i} \geq \langle e_{oc}(j), f_{oc}(j) - r_{oc}(j) \rangle_{N_j}$$

which can be rewritten as

$$\langle f_{op}(i), r_{op}(i) \rangle_{N_i} + \langle e_{oc}(j), r_{oc}(j) \rangle_{N_j} \geq \langle f_{op}(i), e_{op}(i) \rangle_{N_i} + \langle e_{oc}(j), f_{oc}(j) \rangle_{N_j} \quad (41)$$

so that we can then substitute (39) and (40) to yield

$$\langle f_{op}(i), r_{op}(i) \rangle_{N_i} + \langle e_{oc}(j), r_{oc}(j) \rangle_{N_j} \geq \epsilon (\| (f_{op}(i))_{N_i} \|_2^2 + \| (e_{oc}(j))_{N_j} \|_2^2) - \beta \quad (42)$$

in which $\epsilon = \min(\epsilon_{op}, \epsilon_{oc})$ and $\beta = \beta_{op} + \beta_{oc}$. Thus (42) satisfies [13, Definition 3-II] when $i = j$ in which the input is the row vector of $[r_{op}, r_{oc}]$, and the output is the row vector $[f_{op}, e_{oc}]$.

Interestingly, we can describe the controllers behavior in terms of i since the PATRU only transfers data to the controller when available from the plant or sends a 0 to the plant when no control data is available. Equivalently we can simply transfer a 0 to the controller when no data is available from the plant and use a switched controller G_c in which $G_c = G_{co}$ when data is present from the plant and set $G_c = 0$ when the PATRU fills in the missing data for $v_{oc}(i)$, $v_{op}(i)$, and $e_{oc}(i)$ with 0.

Theorem 1. *Using the PATRU as defined by Definition 4 in the control network depicted in Figure 7. The digital control network in Figure 7 is strictly-output passive.*

Proof 5. *From lemma 4 we have shown that (38) holds. Given definition 4, both*

$$\| (e_{oc}(j))_{N_j} \|_2^2 = \| (e_{oc}(i))_{N_i} \|_2^2 \quad (43)$$

and

$$\langle e_{oc}(j), r_{oc}(j) \rangle_{N_j} = \langle e_{oc}(i), r_{oc}(i) \rangle_{N_i} \quad (44)$$

will hold, therefore,

$$\langle f_{op}(i), r_{op}(i) \rangle_{N_i} + \langle e_{oc}(i), r_{oc}(i) \rangle_{N_i} \geq \epsilon (\| (f_{op}(i))_{N_i} \|_2^2 + \| (e_{oc}(i))_{N_i} \|_2^2) - \beta \quad (45)$$

holds in which $\epsilon = \min(\epsilon_{op}, \epsilon_{oc})$ and $\beta = \beta_{op} + \beta_{oc}$.

4. Conclusions

We have presented several results related to digital control of continuous *passive* plants over wireless networks. Of particular importance is that we provided a much needed analysis which captured time varying delays (Lemma 1) and data dropouts (Lemma 2) for two way wireless digital communication token passing medium access control (MAC) networks. Also we showed how a *novel* asynchronous controller can be used to maintain an l^2 -stable system (Theorem 1) while improving control performance over synchronous controllers which rely on lossy data reduction LDR algorithms. More specifically: (i) the *passive* plant (station $m = 2(n - 1)$) and *passive* controller (station $m/2$) were treated as stations of a n node token ring network depicted in Figure 2; (ii) we provided a Markov chain (with transition matrix (6) and Lemma 1) in order to determine the network capacity, mean round trip travel time (τ_m) and variance of travel time for a packet of data in a ring network; (iii) we accounted for the overhead of the data acknowledge, header, and frame control sequence with the corresponding definition for *data capacity* (Definition 2); (iv) Definition 2 (and a useful analysis relating packet error rate to node spacing with wireless transceivers such as the CC2420 in [11, Appendix C.2]) allows one to generate figures such as: a) Figure 3(a) showing the maximum data capacity is attained by sending the longest possible packet until a distance spacing of the nodes is such that p is fairly low, b) and Figure 3(b) shows that a maximum spacing exists which provides the maximum data capacity \times distance for relaying data over a network; (v) in order to account for queuing delays and data dropouts we provide a more precise networking delay model in Lemma 2; (vi) Lemma 2 shows that the delay will undergo a *phase* shift in which the delay will suddenly increase at a critical number of nodes and node separation distance, as seen in Figure 4(a) and verified by simulation in Figure 4(b) such that (a) the sudden increase in delay is equal to the maximum allowed buffer delay D and it occurs when the data rate $r < \frac{1}{\lambda_p} = \frac{2(n-1)}{p}$, (b) this is intuitive since once data is generated at a rate that exceeds the capacity of the network, then the delay will continue to grow unbounded until packets are dropped which occurs when the First-In, First-Out (FIFO) buffer is full.

In order to evaluate control performance over our *passive* wireless network we: (i) introduced a new definition for distortion Definition 3 which allowed us to evaluate and compare: (a) an adaptive LDR algorithm as described in [11, Section 4.3.1] which has been shown to be *passive* [11, Lemma 8], (b) a *novel strictly-output passive* asynchronous controller as depicted in Figure 7 which only computes a new possibly non-zero control command when valid data from the plant is received (Section 3.2); (ii) provided a new Theorem 1 (with corresponding new Lemma 4, and Lemma 3) showing that the asynchronous controller, governed by the PATRU as defined by Definition 4, is indeed *strictly-output passive*; (iii) Figure 6(b) shows the corresponding improvement in distortion for the asynchronous controller, as compared to the one which uses the adaptive compression scheme as shown in Figure 5(b). (iv) using the network models discussed for token ring networks, it should be a fairly straight forward task to design a estimate of the network capacity in order to allow the plant to adjust its sampling rate T_s in order to generate data packets at a rate $r = \frac{1}{\lambda_p}$. This additional piece of information T_s can be sent along to the controller in order to use the appropriate gains to calculate a new control command.

REFERENCES

1. Robert J. Anderson and Mark W. Spong. Bilateral control of teleoperators with time delay. *IEEE Transactions*

- on *Automatic Control*, 34(5):494 – 501, 1989. Bilateral Control;Nonlinear Teleoperation System;Time Delay Caused Instability;.
2. Robert J. Anderson and Mark W. Spong. Asymptotic stability for force reflecting teleoperators with time delay. *International Journal of Robotics Research*, 11(2):135 – 149, 1992. Force-reflecting teleoperators;Master manipulator;Slave manipulator;Transmission delay;Hilbert network;.
 3. P. Berestesty, N. Chopra, and M.W. Spong. Theory and experiments in bilateral teleoperation over the internet. In *Proceedings of the 2004 IEEE International Conference on Control Applications (IEEE Cat. No.04CH37596)*, volume Vol.1, pages 456 – 63, Taipei, Taiwan, 2004.
 4. Paul Berestesty, Nikhil Chopra, and Mark W. Spong. Discrete time passivity in bilateral teleoperation over the internet. *Proceedings - IEEE International Conference on Robotics and Automation*, 2004(5):4557 – 4564, 2004.
 5. Jean-Chrysostome Bolot. End-to-end packet delay and loss behavior in the internet. *Computer Communications Review*, 23(4):289 –, 1993.
 6. Charles A. Desoer and M. Vidyasagar. *Feedback Systems: Input-Output Properties*. Academic Press, Inc., Orlando, FL, USA, 1975.
 7. M. Ergen, Duke Lee, Raja Sengupta, and P. Varaiya. Wtrp - wireless token ring protocol. *IEEE Transactions on Vehicular Technology*, 53(6):1863 – 81, 2004/11/.
 8. X. Fan, K. Chandrayana, M. Arcak, S. Kalyanaraman, and J. T. Wen. A two-time scale design for detection and rectification of uncooperative network flows. *Proceedings of the 44th IEEE Conference on Decision and Control, and the European Control Conference 2005*, pages 1842–1847, December 12-15 2005.
 9. Oscar Flårdh, Karl H. Johansson, and Mikael Johansson. A new feedback control mechanism for error correction in packet-switched networks. *Proceedings of the 44th IEEE Conference on Decision and Control, and the European Control Conference 2005*, pages 488–493, December 12-15 2005.
 10. Texas Instruments. *CC2420: 2.4 GHz; IEEE 802.15.4/ ZigBee-ready RF Transceiver - Data Manual (SWRS041B)*, 2007.
 11. Nicholas Kottenstette. *Control of Passive Plants With Memoryless Nonlinearities Over Wireless Networks*. PhD thesis, University of Notre Dame, August 2007.
 12. Nicholas Kottenstette and Panos Antsaklis. Digital control networks for continuous passive plants which maintain stability using cooperative schedulers. Technical Report isis-2007-002, University of Notre Dame, March 2007.
 13. Nicholas Kottenstette and Panos J. Antsaklis. Stable digital control networks for continuous passive plants subject to delays and data dropouts. *Proceedings of the 46th IEEE Conference on Decision and Control*, pages 4433 – 4440, 2007.
 14. M. Kuschel, P. Kremer, S. Hirche, and M. Buss. Lossy data reduction methods for haptic telepresence systems. In *Proceedings. 2006 Conference on International Robotics and Automation (IEEE Cat. No. 06CH37729D)*, pages 2933 – 8, Orlando, FL, USA, 2006.
 15. Kelvin K. Lee and Samuel T. Chanson. Packet loss probability for bursty wireless real-time traffic through delay model. *IEEE Transactions on Vehicular Technology*, 53(3):929 – 938, 2004.
 16. F. L. Lewis. Optimal control. In W. S. Levine, editor, *The Control Handbook*, pages 759–778. CRC Press, Boca Raton, FL, 1996.
 17. J. Linares-Flores, J. Reger, and H. Sira-Ramirez. A time-varying linear state feedback tracking controller for a boost-converter driven dc motor. *Mechatronics 2006. 4th IFAC Symposium on Mechatronic Systems. Preprints*, pages 926 – 31, 2006/.
 18. Ivana Maric and Roy D. Yates. Cooperative multicast for maximum network lifetime. *IEEE Journal on Selected Areas in Communications*, 23(1):127 – 135, 2005.
 19. Gunter Niemeyer and Jean-Jacques E. Slotine. Telemanipulation with time delays. *International Journal of Robotics Research*, 23(9):873 – 890, 2004.
 20. J. Rosen and B. Hannaford. A doc at a distance [remotely-controlled surgical robots]. *IEEE Spectrum*, 43(10):34 – 9, 2006/10/.
 21. Jee-Hwan Ryu, Yoon Sang Kim, and B. Hannaford. Sampled- and continuous-time passivity and stability of virtual environments. *IEEE Transactions on Robotics*, 20(4):772 – 6, 2004/08/.
 22. J. Laurie Snell. Finite markov chains and their applications. *The American Mathematical Monthly*, 66(2):99–104, February 1959.
 23. S. Stramigioli, C. Secchi, A.J. van der Schaft, and C. Fantuzzi. A novel theory for sampled data system passivity. *Proceedings IEEE/RSJ International Conference on Intelligent Robots and Systems (Cat. No.02CH37332C)*, vol.2:1936 – 41, 2002/.
 24. Arjan van der Schaft. *L2-Gain and Passivity in Nonlinear Control*. Springer-Verlag New York, Inc., Secaucus, NJ, USA, 1999.
 25. Xiaoyi Wu and Christos G. Cassandras. A maximum time optimal control approach to routing in sensor networks. In *Proceedings of the 44th IEEE Conference on Decision and Control, and the European Control Conference 2005*, pages 1137–1142, 2005.
 26. Min Xie and Martin Haenggi. Delay-reliability tradeoffs in wireless networked control systems. In *Workshop on Networked Embedded Sensing and Control*, Lecture Notes in Control and Information Sciences. Springer, October 2005.
 27. Min Xie and Martin Haenggi. A study of the correlations between channel and traffic statistics in multihop networks. *To appear IEEE Transactions on Vehicular Technology*, 2007.

28. Min Xie and Martin Haenggi. Towards an end-to-end delay analysis of wireless multihop networks. In *submitted Ad Hoc Networks*. Elsevier, 2007.

APPENDIX

I. Key Formulas For Finite Markov Chains

We summarize some key results given by [22] as they allow us to evaluate various random processes which can be described by a finite Markov Chain. We assume the chain can be described by a finite set of states $s \in \{1, \dots, m\}$ and the state transition matrix P . If the chain is an absorbing chain, it will reach an absorbing state with probability 1. An absorbing state is one that once reached, it will not leave that state (i.e. $P_{(i,i)} = 1$). Hence, we are interested in the following processes:

1. u_j : The number of times the process is in the nonabsorbing state j before being absorbed.
2. v : The number of steps taken before absorption.
3. w : The number of different nonabsorbing states entered before absorption.
4. x : The state in which the process is absorbed.

Using the following notation:

1. $\Pr_i[p]$: The probability that p occurs when the process is started in state i .
2. $M_i[f]$: The mean value of the random variable f when the process started in state i .
3. $C_i[f, g]$: The covariance of f and g when the process is started in state i .

The transition matrix can be put in a canonical form P in which the absorbing states are placed first such that

$$P = \begin{bmatrix} I & \mathbf{0} \\ R & Q \end{bmatrix} \quad (46)$$

From which we can compute the following first and second moments based on the fundamental matrix $N = (I - Q)^{-1}$ as given in Table III.

Table III. FIRST AND SECOND MOMENT STATISTICS FOR AN ABSORBING MARKOV CHAIN [22]

First Moment	Second Moment
$N = \{M_i[u_j]\} = (I - Q)^{-1}$	$N_2 = \{M_i[u_j^2]\} = N(2N_{dg} - I)$
$\tau = \{M_i[v]\} = Ne$	$\tau_2 = \{M_i[v^2]\} = (2N - I)Ne$
$H = \{M_i[w]\} = NN_{dg}^{-1}e$	

In which N_{dg} is a matrix with the same diagonal elements as N and 0 elsewhere, and e is a column vector of ones. It is also given that $B = \{\Pr_i[x = j]\} = NR$. Denoting the variance of v given i as $\sigma_v^2 = \{C_i[v, v]\}$ can be calculated as follows:

$$\sigma_v^2 = \tau_2 - \text{diag}(\tau)\tau = [2N - I - \text{diag}(Ne)]Ne = [2N - I - \text{diag}(\tau)]\tau. \quad (47)$$

II. Passive Systems, IPESH, and Wave Variables

This appendix provides a brief review of *passive* systems, the *IPESH*, wave variables, and nomenclature to aid in the reading of Section 3.3.

II.1. Passive Systems

The following is a brief summary on *passive* systems. The interested reader is referred to [6, 24] for additional information. Let \mathbb{Z}^+ represent the set of positive integers to indicate time for discrete time signals. l_2^m denotes the space of all discrete time functions $u : \mathbb{Z}^+ \rightarrow \mathbb{R}^m$ which satisfy the following:

$$\|u\|_2^2 = \sum_0^\infty u^T(i)u(i) < \infty. \quad (48)$$

Similarly l_{2e}^m denotes the extended space of discrete time functions $u : \mathbb{Z}^+ \rightarrow \mathbb{R}^m$ which satisfy the following:

$$\|u_N\|_2^2 = \langle u, u \rangle_N = \sum_0^{N-1} u^T(i)u(i) < \infty; \forall N \in \mathbb{Z}^+. \quad (49)$$

Definition 5. A dynamic system $H : l_{2e}^m \rightarrow l_{2e}^m$ is l_2^m stable if

$$x \in l_2^m \implies Hx \in l_2^m. \quad (50)$$

Definition 6. Let $H : l_{2e}^m \rightarrow l_{2e}^m$. We say that H is

i) *passive* if $\exists \beta$ s.t.

$$\langle Hu, u \rangle_N \geq -\beta, \forall u \in l_{2e}^m, \forall N \in \mathbb{Z}^+ \quad (51)$$

ii) *strictly-input passive* if $\exists \delta > 0$ and $\exists \beta$ s.t.

$$\langle Hu, u \rangle_N \geq \delta \|u_N\|_2^2 - \beta, \forall u \in l_{2e}^m, \forall N \in \mathbb{Z}^+ \quad (52)$$

iii) *strictly-output passive* if $\exists \epsilon > 0$ and $\exists \beta$ s.t.

$$\langle Hu, u \rangle_N \geq \epsilon \|Hu_N\|_2^2 - \beta, \forall u \in l_{2e}^m, \forall N \in \mathbb{Z}^+ \quad (53)$$

iv) *non-expansive* if $\exists \hat{\gamma} > 0$ and $\exists \hat{\beta}$ s.t.

$$\|Hu_N\|_2^2 \leq \hat{\beta} + \hat{\gamma}^2 \|u_N\|_2^2, \forall u \in l_{2e}^m, \forall N \in \mathbb{Z}^+ \quad (54)$$

Remark 6. A non-expansive system H is equivalent to any system which has finite l_2^m gain in which there exists constants γ and β s.t. $0 < \gamma < \hat{\gamma}$ and satisfy

$$\|Hu_N\|_2 \leq \gamma \|u_N\|_2 + \beta, \forall u \in l_{2e}^m, \forall N \in \mathbb{Z}^+. \quad (55)$$

Furthermore a non-expansive system implies l_2^m stability [13, Remark 1].

II.2. IPESH

We recall the definition stated in [13, Definition 4] for the *inner-product equivalent sample and hold (IPESH)* depicted in Figure 7 consist of a zero order hold (ZOH) block and *inner-product equivalent sample* block (IPES).

Definition 7. [21, 23] Let a continuous one-port plant be denoted by the input-output mapping $G_{ct} : L_{2e}^m \rightarrow L_{2e}^m$. Denote continuous time as t , the discrete time index as i , the periodic sample rate as T_s , the continuous input as $u(t) \in L_{2e}^m$, the continuous output as $y(t) \in L_{2e}^m$, the transformed discrete input as $u(i) \in l_{2e}^m$, and the transformed discrete output as $y(i) \in l_{2e}^m$. The inner-product equivalent sample and hold (IPESH) is implemented as follows:

- I. $x(t) = \int_0^t y(\tau) d\tau$
- II. $y(i) = x((i+1)T_s) - x(iT_s)$
- III. $u(t) = u(i), \forall t \in [iT_s, i(T_s+1))$

As a result

$$\langle y(i), u(i) \rangle_N = \langle y(t), u(t) \rangle_{NT_s}, \forall N \geq 1 \quad (56)$$

holds.

II.3. Wave Variables

The wave variables depicted in Figure 7 ($u_{o\{p,c\}}(i), v_{o\{p,c\}}(i)$) allow *effort* and *flow* variables to be transmitted over a network while remaining *passive* when subject to arbitrary fixed time delays and data dropouts [19].

$$u_{op}(i) = \frac{1}{\sqrt{2b}}(bf_{op}(i) + e_{doc}(i)) \quad (57)$$

$$v_{oc}(j) = \frac{1}{\sqrt{2b}}(bf_{opd}(j) - e_{oc}(j)) \quad (58)$$

When actually implementing the wave variable transformation the "outputs" (u_{pk}, e_{dock}) are related to the corresponding "inputs" (v_{pk}, f_{opk}) as follows (see [11, Figure 2.2]):

$$\begin{bmatrix} u_{op}(i) \\ e_{doc}(i) \end{bmatrix} = \begin{bmatrix} -I & \sqrt{2b}I \\ -\sqrt{2b}I & bI \end{bmatrix} \begin{bmatrix} v_{op}(i) \\ f_{op}(i) \end{bmatrix} \quad (59)$$

likewise the "outputs" (v_{oc}, f_{opd}) are related to the corresponding "inputs" (u_{oc}, e_{oc}) as follows:

$$\begin{bmatrix} v_{oc}(j) \\ f_{opd}(j) \end{bmatrix} = \begin{bmatrix} I & -\sqrt{\frac{2}{b}}I \\ \sqrt{\frac{2}{b}}I & -\frac{1}{b}I \end{bmatrix} \begin{bmatrix} u_{oc}(j) \\ e_{oc}(j) \end{bmatrix}. \quad (60)$$